

# Generative Frontier Planning for Adaptive Peer-Referral Recruitment under Covariate-Dependent Arrivals

Lingkai Kong\*  
Harvard University  
Cambridge, Massachusetts, USA  
lingkaikong@g.harvard.edu

Hezi Jiang\*  
Harvard University  
Cambridge, Massachusetts, USA  
hjiang26@g.harvard.edu

Andrew Ma  
Harvard University  
Cambridge, Massachusetts, USA  
andrewma@g.harvard.edu

Keyu Wang  
Harvard University  
Cambridge, Massachusetts, USA  
keyuwang@g.harvard.edu

Akseli Kangaslahti  
Harvard University  
Cambridge, Massachusetts, USA  
akselikangaslahti@g.harvard.edu

Milind Tambe  
Harvard University  
Cambridge, Massachusetts, USA  
milind\_tambe@harvard.edu

## Abstract

Peer-referral recruitment systems such as respondent-driven sampling are critical for studying and intervening on hidden populations affected by infectious diseases. To accelerate recruitment, public health agencies must adaptively allocate limited referral resources across multiple rounds, where current decisions shape both the number and the covariates of future recruits. Prior work makes this problem tractable by assuming that referrals are drawn i.i.d. from a homogeneous population, an assumption that ignores the homophily and shared context that drive real peer recruitment. We instead consider a more realistic model in which both referral capacity and the covariates of newly referred individuals are conditioned on the referrer, learned from data with a censored count model and a conditional generative model. The resulting planning problem is challenging because each candidate allocation induces a different distribution over future recruits. We propose *Generative Frontier Planning* (GFP), a model-based planner that replaces per-step Monte-Carlo sampling with a deterministic backup over a latent covariate-coverage value surrogate. The surrogate is designed so that the expected value of the next frontier depends on the offspring generative model only through finite-dimensional summaries that are amortized offline, and so that the resulting per-round objective is monotone with diminishing returns. Together, these two properties make planning tractable: the deterministic backup eliminates Monte-Carlo sampling, and the diminishing-returns structure lets a marginal greedy allocation achieve a  $(1 - 1/e)$ -approximation for the per-round problem. On a simulation environment calibrated to a real respondent-driven sampling dataset, GFP outperforms random, reinforcement-learning, and i.i.d. dynamic-programming baselines across four discount factors.

## 1 Introduction

Peer-referral recruitment systems such as respondent-driven sampling (RDS) [10] and incentivized contact tracing [17] are crucial tools for studying and preventing the spread of infectious diseases. In these settings, enrolled individuals recursively refer their peers into the study, enabling public health agencies to learn about behavior, disease prevalence, and population structure—especially in “hidden” populations that are otherwise largely unobserved and underserved [12]. The resulting recruitment data are also valuable for informing downstream decisions about limited intervention resources [5, 14].

To encourage participation, public health agencies distribute limited resources, such as referral vouchers or monetary incentives, to enrolled individuals. Because peer recruitment unfolds recursively over time, the decision-maker can split a fixed total budget into multiple rounds, adapting to the observed “frontier” of active recruits as recruitment proceeds. Individuals themselves also act adaptively: the number of peers they refer can depend on the amount of resources they receive. Public health agencies must therefore design adaptive allocation strategies that reason about complex referral dynamics in order to recruit as many individuals as possible as quickly as possible.

Although this problem has been studied in prior work [19], that formulation assumes that referrals for newly recruited individuals are drawn i.i.d. from a fixed population-level distribution. Under this assumption, the value of a recruitment frontier depends only on its size. This is mathematically convenient but ignores dependence between referrers and their referees, which is unrealistic in practice: peer referrals are shaped by homophily, geographic proximity, and shared behavioral context. We address this limitation with a more realistic data-driven model in which referral dynamics are conditioned on referrer covariates, drawing on recent generative models of infectious-disease recruitment [14].

Under this modeling shift, planning becomes substantially more challenging. The value of a frontier now depends not only on its size but also on its covariate composition, so prior allocation algorithms that summarize a frontier by frontier size alone become suboptimal. Beyond this, model-based planning faces two coupled obstacles. First, computing the expected value of the next frontier has no closed form: the next frontier is a variable-size random set whose elements are drawn from a generative offspring model, so

\*Both authors contributed equally to this research.

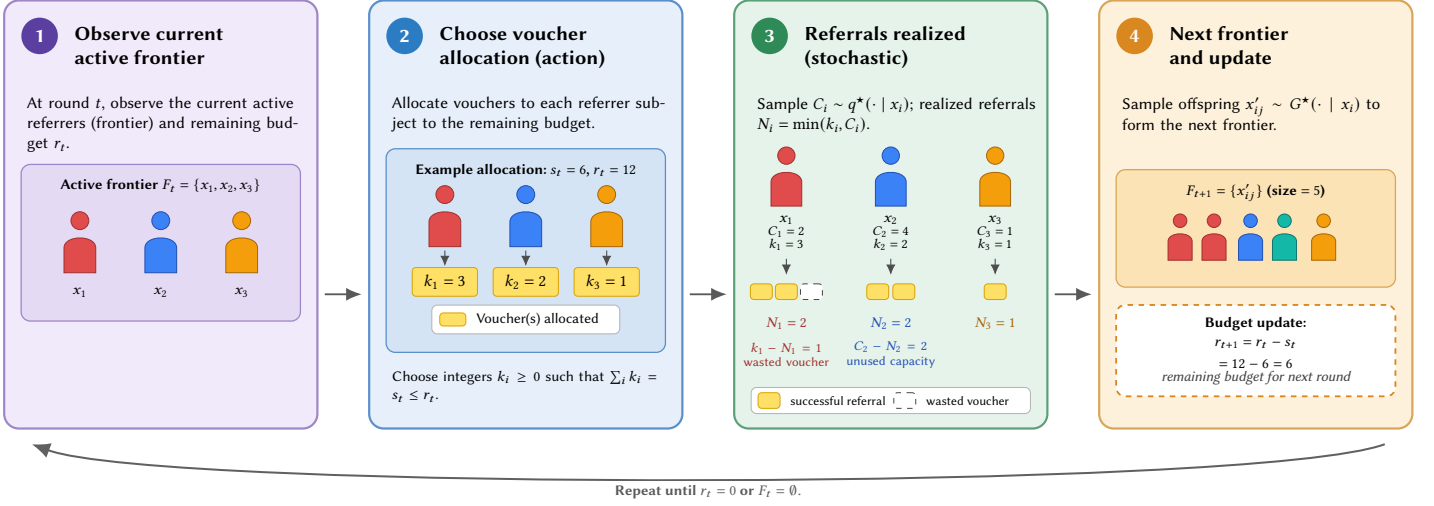


**Figure 1: Sequential decision process for adaptive peer-referral recruitment.** Starting from an initial frontier  $F_0$  and total budget  $B$ , at each round  $t$  the decision-maker observes the current frontier  $F_t = \{x_1, \dots, x_n\}$  and remaining budget  $r_t$  (with  $r_0 = B$ ), then allocates referral vouchers  $k_i \geq 0$  to each active referrer subject to  $\sum_i k_i = s_t \leq r_t$ . Each referrer  $i$  has a stochastic referral capacity  $C_i \sim q^*(\cdot | x_i)$ , and the realized number of successful referrals is the capped count  $N_i = \min(k_i, C_i)$ . Conditioned on the parent covariate  $x_i$ , the referrer generates  $N_i$  offspring with covariates sampled independently as  $x'_{ij} \sim G^*(\cdot | x_i)$  for  $j = 1, \dots, N_i$ , which together form the next frontier  $F_{t+1} = \{x'_{ij}\}$ . The budget then updates as  $r_{t+1} = r_t - s_t$ , and the process repeats until  $r_t = 0$  or  $F_t = \emptyset$ . Each color represents a simplified covariate vector summarizing demographic, behavioral, or geographic attributes. Different allocations  $k_t$  induce different offspring distributions, so current decisions shape both the size *and* the covariate composition of future frontiers. The goal is to maximize the expected (discounted) number of successful referrals over the horizon.

the expectation must in principle be estimated by Monte-Carlo sampling. Second, since different allocations induce different offspring distributions, these samples cannot be shared across candidate allocations, and the per-round action space (integer allocations across all frontier individuals) is itself combinatorially large. Together, these obstacles make naive model-based planning intractable.

In this work, we propose a model-based planning method that addresses both obstacles. We learn referral dynamics with a censored count model and a conditional diffusion model of offspring covariates, and combine them with a budget-conditioned value surrogate over latent covariate coverage. The surrogate is designed so that two properties hold simultaneously. First, its expected future value depends on the diffusion model only through finite-dimensional summaries of the offspring distribution (the conditional Laplace embeddings) that are amortized offline; the resulting Bellman backup is fully deterministic and shared across candidate allocations, eliminating per-step Monte-Carlo sampling. Second, the induced per-round objective is monotone with diminishing returns, so a marginal greedy allocation achieves a  $(1 - 1/e)$ -approximation despite the combinatorial action space.

We summarize our contributions as follows:

- (1) We formalize peer-referral recruitment as adaptive multi-round resource allocation in which both the number and the covariates of future arrivals are generated conditional on the current allocation and frontier, generalizing prior i.i.d. population-level formulations [19].

- (2) We propose *Generative Frontier Planning* (GFP), a model-based planner that combines a learned censored count model and a learned conditional diffusion model of offspring covariates with a latent-coverage value surrogate. Using conditional Laplace embeddings of the offspring model, GFP evaluates expected future values in closed form, replacing per-step Monte-Carlo sampling with a deterministic backup that is used identically for planning and fitted-value-iteration training.
- (3) We prove that the resulting surrogate is monotone with integer diminishing returns, giving a  $(1 - 1/e)$ -approximation guarantee for the per-round allocation. Empirically, on a simulation environment calibrated to a real respondent-driven sampling dataset, GFP outperforms random allocation, reinforcement learning baselines, and an i.i.d. population-level dynamic-programming baseline across four discount factors.

## 2 Problem Formulation

We formulate adaptive multi-round peer-referral recruitment as a finite-horizon planning problem with a total budget  $B$  allocated across rounds. We use  $t = 0, 1, 2, \dots$  to index rounds and suppress the round index when describing the per-round mechanics below; subscripts in  $t$  reappear only in the multi-round objective.

*State and action.* At the current round, the decision-maker observes a frontier of active individuals

$$\mathcal{F} = \{\mathbf{x}_1, \dots, \mathbf{x}_n\},$$

where  $\mathbf{x}_i \in \mathcal{X}$  denotes the covariate vector of individual  $i$  (e.g., demographic, behavioral, geographic, or network features) and the frontier size  $n = |\mathcal{F}|$  varies across rounds. The remaining budget  $r \in \mathbb{N}_0$  is initialized to  $r_0 = B$ , where  $\mathbb{N}_0 = \{0, 1, 2, \dots\}$ .

An action consists of a round budget

$$s \in \{0, \dots, r\}$$

and an integer allocation vector

$$\mathbf{k} = (k_1, \dots, k_n) \in \mathbb{N}_0^n, \quad \sum_{i=1}^n k_i = s,$$

where  $k_i$  is the number of referral resources assigned to individual  $i$ ; the case  $s = 0$  corresponds to assigning no resources in the current round.

*Referral capacity.* Each frontier individual  $i$  has a stochastic referral capacity

$$C_i \sim q^*(\cdot | \mathbf{x}_i),$$

where  $q^*$  is an unknown conditional count distribution. Given allocation  $k_i$ , the realized number of successful referrals is the capped count

$$N_i(k_i) = \min\{k_i, C_i\}.$$

The immediate reward in the current round is therefore

$$R(\mathcal{F}, \mathbf{k}; C) = \sum_{i=1}^n N_i(k_i), \quad C = (C_1, \dots, C_n).$$

Because each individual's output is capped at the realized capacity  $C_i$ , any units assigned beyond  $C_i$  are wasted; equivalently, the expected per-unit yield  $\Pr_{C \sim q^*(\cdot | \mathbf{x}_i)}(C \geq \ell)$  is nonincreasing in  $\ell$ .

*Covariate-dependent generative arrivals.* In contrast to population-level arrival models in which newly referred individuals are sampled i.i.d. from a fixed population distribution, we assume that offspring covariates depend on the referrer. Conditional on  $N_i(k_i)$ , the covariates of individual  $i$ 's referrals are drawn as

$$\mathbf{x}'_{ij} \sim G^*(\cdot | \mathbf{x}_i), \quad j = 1, \dots, N_i(k_i),$$

where  $G^*$  is an unknown parent-conditioned offspring covariate distribution. The next frontier is the random set

$$\mathcal{F}' = \{\mathbf{x}'_{ij} : i \in \{1, \dots, n\}, j = 1, \dots, N_i(k_i)\}.$$

This captures the fact that referrals are not drawn from a homogeneous population: individuals tend to recruit others whose covariates are shaped by their own social, geographic, demographic, or behavioral context.

*Policy and objective.* A policy  $\pi$  maps each state  $(r, \mathcal{F})$  to a feasible action  $(s, \mathbf{k})$ . After executing  $(s, \mathbf{k})$ , the budget evolves deterministically as  $r' = r - s$ , and the next frontier  $\mathcal{F}'$  is generated according to  $q^*$  and  $G^*$ . The objective is to maximize the expected discounted number of successful referrals,

$$V^\pi(r, \mathcal{F}) = \mathbb{E}_\pi \left[ \sum_{t \geq 0} \gamma^t R(\mathcal{F}_t, \mathbf{k}_t; C_t) \mid r_0 = r, \mathcal{F}_0 = \mathcal{F} \right],$$

with discount factor  $\gamma \in (0, 1]$  and the terminal convention  $V^\pi(0, \mathcal{F}) = V^\pi(r, \emptyset) = 0$ , since no further successful referrals can be generated once the budget is exhausted or the frontier is empty.

### 3 Proposed Method

We propose *Generative Frontier Planning* (GFP), a model-based approximate dynamic programming method for adaptive multi-round allocation under covariate-dependent arrivals. The method proceeds in three steps. Section 3.1 introduces the learned referral dynamics and explains why generic model-based fitted value iteration is intractable. Section 3.2 introduces a structured value surrogate whose Bellman backup admits a closed-form expression through conditional Laplace embeddings of the offspring distribution. Section 3.3 describes intra-round greedy allocation under the resulting deterministic surrogate and gives the fixed-budget approximation guarantee. Section 3.4 describes how the surrogate is fitted using the same closed-form backup.

#### 3.1 Model-Based Value Fitting and Its Computational Bottleneck

GFP is a model-based planner: the true dynamics  $q^*$  and  $G^*$  are unknown, so we plan with learned surrogates  $q_\psi$  and  $G_\theta$  estimated offline from historical referral data.

*Learning referral dynamics.* GFP uses two learned components: a conditional referral-capacity model  $q_\psi(c | \mathbf{x}) \approx q^*(c | \mathbf{x})$ , and a conditional offspring covariate model  $G_\theta(\mathbf{x}' | \mathbf{x}) \approx G^*(\mathbf{x}' | \mathbf{x})$ .

The first models the stochastic referral capacity  $C_i$  of an individual with covariates  $\mathbf{x}_i$ . In referral systems, the observed number of successful referrals is censored by the allocated budget: if individual  $i$  receives  $k_i$  resources and generates  $y_i$  successful referrals, then  $y_i = \min\{C_i, k_i\}$ . We therefore fit  $q_\psi$  under the censored likelihood

$$\mathbb{P}(Y_i = y_i | \mathbf{x}_i, k_i) = \begin{cases} q_\psi(y_i | \mathbf{x}_i), & y_i < k_i, \\ \mathbb{P}_{C \sim q_\psi(\cdot | \mathbf{x}_i)}(C \geq k_i), & y_i = k_i, \end{cases}$$

which avoids treating saturated observations  $y_i = k_i$  as evidence that the true capacity equals  $k_i$ . In our implementation,  $q_\psi$  is a neural Poisson regression model whose rate depends on the parent covariates.

The second models the covariates of newly referred individuals. Given a parent covariate vector  $\mathbf{x}$ , the offspring covariate vector  $\mathbf{x}'$  is drawn from  $G_\theta(\cdot | \mathbf{x})$ . We instantiate  $G_\theta$  as a conditional diffusion model [13] over the covariate space  $\mathcal{X}$ , which provides a flexible generative model for high-dimensional covariates. Other conditional generative models (e.g., conditional normalizing flows [22]) could be substituted without changing the rest of the framework.

*Generic model-based fitted value iteration.* A natural way to use the learned models is fitted value iteration. Given a value function  $V_\phi(r, \mathcal{F})$ , the model-based Bellman backup decomposes into an expected immediate reward and an expected future value:

$$(\mathcal{T}V_\phi)(r, \mathcal{F}) = \max_{0 \leq s \leq r} \max_{\mathbf{k} \in \mathbb{N}_0^n: \sum_i k_i = s} \left\{ A_\psi(\mathcal{F}, \mathbf{k}) + \gamma \mathbb{E} [V_\phi(r - s, \mathcal{F}')] \right\}, \quad (1)$$

where the expected immediate reward is

$$A_\psi(\mathcal{F}, \mathbf{k}) = \sum_{i=1}^n \sum_{\ell=1}^{k_i} p_{\psi,i}(\ell), \quad (2)$$

with survival probability  $p_{\psi,i}(\ell) := \mathbb{P}_{C \sim q_\psi(\cdot | \mathbf{x}_i)}(C \geq \ell)$ , and the future-value expectation is over  $C_i \sim q_\psi(\cdot | \mathbf{x}_i)$ ,  $N_i = \min\{k_i, C_i\}$ , and offspring covariates  $\mathbf{x}'_{ij} \sim G_\theta(\cdot | \mathbf{x}_i)$  forming the next frontier  $\mathcal{F}' = \{\mathbf{x}'_{ij} : i = 1, \dots, n, j = 1, \dots, N_i\}$ .

The immediate-reward term  $A_\psi(\mathcal{F}, \mathbf{k})$  decomposes additively over individuals and is closed form:  $p_{\psi,i}(\ell)$  is the probability that the  $\ell$ -th unit assigned to individual  $i$  is not wasted. The expected-future-value term, by contrast, is intractable. Computing the Bellman backup faces three coupled challenges:

- (C1) *Random next frontier.* For a generic  $V_\phi$ , the expected future value  $\mathbb{E}[V_\phi(r-s, \mathcal{F}')]$  has no closed form:  $\mathcal{F}'$  is a random set whose size depends on  $\mathbf{k}$  through  $q_\psi$ , and whose elements are drawn from the diffusion model  $G_\theta$ . A Monte-Carlo estimator must sample  $\mathcal{F}'$  and evaluate  $V_\phi$  on the sampled set.
- (C2) *Combinatorial action space.* For each candidate round budget  $s$ , there are  $\binom{s+n-1}{n-1}$  feasible integer allocations, which is prohibitive for the frontier sizes and budgets we consider.
- (C3) *Allocation–expectation coupling.* Different allocations  $\mathbf{k}$  induce different next-frontier distributions, so the Monte-Carlo estimate in (C1) cannot be shared across the action space in (C2): each candidate  $\mathbf{k}$  requires its own offspring samples.

Together, (C1)–(C3) make generic Monte-Carlo fitted value iteration intractable. We resolve all three by choosing a structured value surrogate whose expected future value is a deterministic function of finite-dimensional amortized summaries of  $G_\theta$ , and whose induced fixed-budget objective is monotone with diminishing returns.

### 3.2 Structured Value Surrogate and Closed-Form Backup

We restrict  $V_\phi$  to a structured form that has two key properties: (i) given offline-amortized summaries of  $G_\theta$  and  $q_\psi$ , the expected future value  $\mathbb{E}[V_\phi(r-s, \mathcal{F}')]$  is a deterministic function of  $\mathbf{k}$ , so no per-step Monte-Carlo sampling is required and the same amortized summaries serve every candidate allocation; and (ii) the induced per-round objective is monotone with diminishing returns, which we exploit in Section 3.3 to obtain a  $(1 - 1/e)$ -approximation via marginal greedy allocation. Property (i) addresses (C1) and (C3); property (ii) addresses (C2). We develop property (i) in this section.

*Surrogate definition.* We approximate the value function by

$$V_\phi(r, \mathcal{F}) = F_\phi\left(r, \sum_{\mathbf{x} \in \mathcal{F}} \mathbf{h}_\phi(\mathbf{x})\right), \quad (3)$$

where  $\mathbf{h}_\phi : \mathcal{X} \rightarrow \mathbb{R}_+^d$  maps each individual to a nonnegative latent summary representation, parameterized as  $\mathbf{h}_\phi(\mathbf{x}) = \text{softplus}(\tilde{\mathbf{h}}_\phi(\mathbf{x}))$  with  $\tilde{\mathbf{h}}_\phi$  an unconstrained neural network. Intuitively,  $\mathbf{h}_\phi(\mathbf{x})$  can be read as a soft assignment of individual  $\mathbf{x}$  to  $d$  latent ‘‘covariate prototypes’’; the aggregate  $\sum_{\mathbf{x} \in \mathcal{F}} \mathbf{h}_\phi(\mathbf{x})$  then summarizes, per prototype, how much of that prototype is currently represented in the frontier. A more concrete instance and a worked-out example are given in Appendix A. We instantiate  $F_\phi$  as an exponential-saturation

function over this latent coverage:

$$F_\phi(r, \mathbf{z}) = \sum_{j=1}^d w_{\phi,j}(r) (1 - \exp(-z_j)), \quad (4)$$

with  $w_{\phi,j}(r) \geq 0$ . The budget-dependent weights are parameterized by a small neural network: for  $r > 0$  we set  $\mathbf{w}_\phi(r) = r \cdot \text{softmax}(g_\phi(r)) \in \mathbb{R}_+^d$ , and  $\mathbf{w}_\phi(0) = \mathbf{0}$ , so that  $V_\phi(0, \mathcal{F}) = 0$  and  $0 \leq V_\phi(r, \mathcal{F}) \leq r$ , consistent with the fact that the future number of successful referrals cannot exceed the remaining budget.

This surrogate encodes diminishing returns over latent coverage. The nonnegativity of  $\mathbf{h}_\phi$  implies that adding an individual can only increase the latent coverage vector coordinate-wise, so the value is monotone in the frontier. The concavity of  $1 - \exp(-z)$  makes repeated increases in the same latent coordinate less valuable, capturing redundancy among prototype-similar frontier individuals. The surrogate works best when future value is well explained by how broadly the frontier spans the covariate space, with diminishing returns as individual regions become saturated; it is less appropriate when future value hinges on nonlinear interactions between specific frontier members that go beyond additive latent coverage.

*Conditional Laplace embeddings.* The key quantity that turns the future-value expectation deterministic is, for each parent  $\mathbf{x}_i$  and latent coordinate  $j$ , the *conditional Laplace embedding*

$$\alpha_{\theta,\phi,j}(\mathbf{x}_i) = \mathbb{E}_{\mathbf{y} \sim G_\theta(\cdot | \mathbf{x}_i)} [\exp(-h_{\phi,j}(\mathbf{y}))], \quad (5)$$

with  $\alpha_{\theta,\phi,j}(\mathbf{x}_i) \in (0, 1]$ , collected into a vector  $\boldsymbol{\alpha}_{\theta,\phi}(\mathbf{x}) \in (0, 1]^d$ . This vector summarizes all information from  $G_\theta(\cdot | \mathbf{x})$  needed by the surrogate. Crucially,  $\boldsymbol{\alpha}_{\theta,\phi}(\mathbf{x})$  depends only on the parent covariate  $\mathbf{x}$ , not on the allocation or frontier. We therefore amortize it with an offline-trained network  $L_\eta(\mathbf{x}) \approx \boldsymbol{\alpha}_{\theta,\phi}(\mathbf{x})$  that is fit by sampling offspring from  $G_\theta$  on a fixed set of parent covariates before planning begins. At planning time, evaluating the embedding for a new parent is a single forward pass through  $L_\eta$ ; no sampling from  $G_\theta$  is required inside the Bellman backup.

**PROPOSITION 1 (CLOSED-FORM EXPECTED FUTURE VALUE).** *Fix a frontier  $\mathcal{F} = \{\mathbf{x}_1, \dots, \mathbf{x}_n\}$ , remaining budget  $r$ , round budget  $s \leq r$ , and allocation  $\mathbf{k}$  with  $\sum_i k_i = s$ . Under the offspring model of Section 2 with learned dynamics  $q_\psi, G_\theta$ , the surrogate in Equations (3)–(4), and the conditional Laplace embeddings in Equation (5), the expected value of the next frontier admits the closed form*

$$\mathbb{E}[V_\phi(r-s, \mathcal{F}')] = \sum_{j=1}^d w_{\phi,j}(r-s) \left(1 - \prod_{i=1}^n \tau_{ij}(k_i)\right), \quad (6)$$

where

$$\tau_{ij}(k_i) = \mathbb{E}_{C_i \sim q_\psi(\cdot | \mathbf{x}_i)} \left[ \alpha_{\theta,\phi,j}(\mathbf{x}_i)^{\min\{k_i, C_i\}} \right], \quad (7)$$

with  $\tau_{ij}(0) = 1$ .

Proposition 1 replaces the variable-size random next-frontier expectation with a deterministic function of survival probabilities and Laplace embeddings. Given  $L_\eta$  and the count model  $q_\psi$ , Equation (6) is evaluable without any sampling at planning time:  $\alpha_{\theta,\phi,j}(\mathbf{x}_i)$  is supplied by a forward pass through  $L_\eta$ , and the outer expectation over  $C_i$  in Equation (7) reduces to a finite sum over the support of

$q_\psi(\cdot \mid \mathbf{x}_i)$  (truncated above by  $k_i$ ). The proof, which uses parent-wise independence to factorize  $\mathbb{E}[\exp(-Z'_i)]$  and the conditional independence of offspring covariates given  $N_i$  to reduce each factor to  $\tau_{ij}(k_i)$ , is deferred to Appendix B.

Combining Equation (2) with Proposition 1, the deterministic surrogate Q-value is

$$\tilde{Q}_\phi(r, \mathcal{F}, s, \mathbf{k}) = A_\psi(\mathcal{F}, \mathbf{k}) + \gamma \sum_{j=1}^d w_{\phi,j}(r-s) \left(1 - \prod_{i=1}^n \tau_{ij}(k_i)\right), \quad (8)$$

for  $\sum_i k_i = s$ . Equation (8) is exact for the structured surrogate under the learned models: the approximation lies in restricting  $V^*$  to the form  $V_\phi$ , not in estimating the Bellman expectation by Monte-Carlo sampling.

### 3.3 Intra-Round Greedy Allocation under the Deterministic Surrogate

Given the deterministic surrogate Q-value  $\tilde{Q}_\phi(r, \mathcal{F}, s, \mathbf{k})$ , planning at each round reduces to a two-level optimization: for each candidate round budget  $s \in \{0, \dots, r\}$ , approximately maximize  $\tilde{Q}_\phi$  over integer allocations  $\mathbf{k} \in \mathbb{N}_0^n$  with  $\sum_i k_i = s$ ; then select the round budget whose best allocation has the highest surrogate value. We refer to the inner step as *intra-round* allocation, and to the outer step as *cross-round* budget selection.

*Marginal greedy procedure.* For a fixed  $s$ , write

$$f_s(\mathbf{k}) = A_\psi(\mathcal{F}, \mathbf{k}) + \gamma \sum_{j=1}^d w_{\phi,j}(r-s) \left(1 - \prod_{i=1}^n \tau_{ij}(k_i)\right). \quad (9)$$

Although  $f_s$  is closed form and cheap to evaluate at any given  $\mathbf{k}$ , exactly maximizing it over all feasible allocations is still combinatorial: there are  $\binom{s+n-1}{n-1}$  integer allocations summing to  $s$ , and  $f_s$  is non-separable across individuals through the product  $\prod_i \tau_{ij}(k_i)$ , so per-individual optimization is not valid. GFP therefore uses intra-round marginal greedy. Starting from  $\mathbf{k} = \mathbf{0}$ , let  $u_j(\mathbf{k}) = \prod_{i=1}^n \tau_{ij}(k_i)$  with  $u_j(\mathbf{0}) = 1$ . The marginal gain of assigning one additional resource to individual  $i$  is

$$\Delta_i(\mathbf{k}; s) = p_{\psi,i}(k_i+1) + \gamma \sum_{j=1}^d w_{\phi,j}(r-s) u_j(\mathbf{k}) \left(1 - \frac{\tau_{ij}(k_i+1)}{\tau_{ij}(k_i)}\right), \quad (10)$$

which uses the multiplicative update  $u_j(\mathbf{k} + \mathbf{e}_i) = u_j(\mathbf{k}) \tau_{ij}(k_i+1)/\tau_{ij}(k_i)$ . The first term in Equation (10) is the marginal expected immediate reward; the second term is the marginal contribution to future latent coverage, weighted by the budget-dependent future-value coefficients  $w_{\phi,j}(r-s)$ . GFP selects the individual with the largest marginal gain, increments its allocation, and updates  $u_j$ , repeating until  $s$  resources have been assigned. Let the resulting allocation be  $\mathbf{k}_s$ ; GFP then selects  $s^* \in \arg \max_{0 \leq s \leq r} \tilde{Q}_\phi(r, \mathcal{F}, s, \mathbf{k}_s)$  and executes  $\mathbf{k}_{s^*}$ . Algorithm 1 summarizes the full procedure. In contrast, the greedy in [19] allocates units according to marginal expected immediate reward only, with future value entering exclusively through cross-round budget selection; our marginal gain in Equation (10) additionally accounts for how each unit reshapes the next frontier's covariate composition.

The intra-round greedy step is justified by the diminishing-returns structure induced by the surrogate.

---

#### Algorithm 1 Generative Frontier Planning

---

**Require:** Frontier  $\mathcal{F} = \{\mathbf{x}_1, \dots, \mathbf{x}_n\}$ , remaining budget  $r$ , count model  $q_\psi$ , Laplace network  $L_\eta$ , weights  $\mathbf{w}_\phi$

- 1: **for**  $s = 0, 1, \dots, r$  **do**
- 2:    $\mathbf{k} \leftarrow \mathbf{0}$ ,  $A \leftarrow 0$ ,  $u_j \leftarrow 1$  for all  $j$
- 3:   **for**  $m = 1, \dots, s$  **do**
- 4:     **for**  $i = 1, \dots, n$  **do**
- 5:        $p_i \leftarrow \mathbb{P}_{C \sim q_\psi(\cdot \mid \mathbf{x}_i)}(C \geq k_i + 1)$
- 6:       **for**  $j = 1, \dots, d$  **do**
- 7:          Compute  $\tau_{ij}(k_i)$ ,  $\tau_{ij}(k_i + 1)$  using  $L_\eta(\mathbf{x}_i)$  and  $q_\psi(\cdot \mid \mathbf{x}_i)$
- 8:           $\beta_{ij} \leftarrow \tau_{ij}(k_i + 1)/\tau_{ij}(k_i)$
- 9:       **end for**
- 10:        $\Delta_i \leftarrow p_i + \gamma \sum_j w_{\phi,j}(r-s) u_j(1 - \beta_{ij})$
- 11:     **end for**
- 12:      $i^* \leftarrow \arg \max_i \Delta_i$
- 13:     **for**  $j = 1, \dots, d$  **do**
- 14:        $u_j \leftarrow u_j \cdot \beta_{i^*j}$
- 15:     **end for**
- 16:      $k_{i^*} \leftarrow k_{i^*} + 1$
- 17:      $A \leftarrow A + \mathbb{P}_{C \sim q_\psi(\cdot \mid \mathbf{x}_{i^*})}(C \geq k_{i^*})$
- 18:   **end for**
- 19:    $\mathbf{k}_s \leftarrow \mathbf{k}$
- 20:    $\tilde{Q}_\phi(r, \mathcal{F}, s) \leftarrow A + \gamma \sum_j w_{\phi,j}(r-s)(1 - u_j)$
- 21: **end for**
- 22: **return**  $s^* = \arg \max_{0 \leq s \leq r} \tilde{Q}_\phi(r, \mathcal{F}, s)$  and  $\mathbf{k}_{s^*}$

---

**PROPOSITION 2 (DIMINISHING RETURNS OF THE DETERMINISTIC SURROGATE).** *Assume  $p_{\psi,i}(\ell)$  is nonincreasing in  $\ell$  for every  $i$ ,  $\mathbf{h}_\phi(\mathbf{x}) \in \mathbb{R}_+^d$ , and  $w_{\phi,j}(r-s) \geq 0$ . Then  $\alpha_{\theta,\phi,j}(\mathbf{x}_i) \in (0, 1]$ ,  $\tau_{ij}(k_i)$  is nonincreasing in  $k_i$ , and  $f_s(\mathbf{k})$  is monotone and satisfies integer diminishing returns: for any  $\mathbf{k} \leq \mathbf{k}'$  coordinate-wise and any individual  $i$ ,*

$$f_s(\mathbf{k} + \mathbf{e}_i) - f_s(\mathbf{k}) \geq f_s(\mathbf{k}' + \mathbf{e}_i) - f_s(\mathbf{k}').$$

**PROPOSITION 3 (GREEDY APPROXIMATION FOR FIXED-BUDGET ALLOCATION).** *Under the conditions of Proposition 2, intra-round marginal greedy gives a constant-factor approximation to the best fixed-budget allocation under  $f_s$ . For the cardinality-constrained resource-unit relaxation, greedy achieves the standard  $(1-1/e)$ -approximation:*

$$f_s(\mathbf{k}_{\text{greedy}}) \geq (1-1/e) \max_{\mathbf{k} \in \mathbb{N}_0^n: \sum_i k_i = s} f_s(\mathbf{k}).$$

Propositions 1–3 characterize the gap between GFP's output and the optimal allocation under the structured surrogate. The gap to the true optimal policy can be further decomposed into model estimation error in  $q_\psi$  and  $G_\theta$ , estimation error in the Laplace network  $L_\eta$ , value approximation error from restricting  $V^*$  to  $V_\phi$ , and the fixed-budget greedy approximation error. Proofs of Propositions 2–3 are given in Appendix B.

### 3.4 Fitting the Structured Value Surrogate

We fit the structured value surrogate by fitted value iteration using the same closed-form backup as in planning. Given sampled states

$(r, \mathcal{F})$ , define the target

$$\widehat{\mathcal{T}}V_{\bar{\phi}}(r, \mathcal{F}) = \max_{0 \leq s \leq r} \left[ A_{\psi}(\mathcal{F}, \mathbf{k}_s) + \gamma \sum_{j=1}^d w_{\bar{\phi}, j}(r-s) \left( 1 - \prod_{i=1}^n \tau_{ij}^{\bar{\phi}}(k_{s,i}) \right) \right], \quad (11)$$

where  $\mathbf{k}_s$  is obtained by the intra-round greedy planner using target parameters  $\bar{\phi}$ , and  $\tau_{ij}^{\bar{\phi}}$  is computed from  $\alpha_{\theta, \bar{\phi}, j}(\mathbf{x}_i)$ . The value parameters are updated by minimizing

$$\mathcal{L}_V(\phi) = \mathbb{E}_{(r, \mathcal{F})} \left[ \left( V_{\phi}(r, \mathcal{F}) - \widehat{\mathcal{T}}V_{\bar{\phi}}(r, \mathcal{F}) \right)^2 \right], \quad (12)$$

with target parameters  $\bar{\phi}$  updated periodically. Because both training and deployment use the same deterministic closed-form backup, GFP avoids per-step Monte-Carlo sampling throughout fitted value iteration and planning.

## 4 Related Work

*Adaptive multi-round allocation and budgeted MDPs.* Most closely related to our setting is adaptive multi-round allocation with stochastic arrivals [19], which obtains tractability by assuming i.i.d. population-level future arrivals and summarizing the frontier by its size alone, so that the value function reduces to a table over remaining budget and frontier size. Our method generalizes this framework to covariate-dependent generative arrivals, where the next frontier is drawn conditional on the referrer, and future value therefore depends on covariate composition rather than only on frontier size. More broadly, resource-constrained sequential decision problems are commonly modeled by constrained or budgeted MDPs [3, 4], and large-scale allocation settings with weakly coupled subprocesses motivate decomposition-based planning rather than direct dynamic programming over the full joint state [6, 15]. These formulations typically assume a fixed set of controlled entities; in our setting, allocating resources to the current frontier changes the future set of decision opportunities, resembling a controlled branching process. Branching MDPs formalize such controlled population growth but mainly target extinction or reachability over finite-type populations, rather than budgeted allocation over covariate-composed frontiers [7].

*Approximate dynamic programming for stochastic allocation.* When exact Bellman recursions are ruled out by high-dimensional state spaces, large action sets, or stochastic future arrivals, a common strategy is approximate dynamic programming [1, 2, 8, 20], in which the value function is replaced by a tractable parametric or aggregated surrogate. Classical surrogates include feature-based value approximation [21] and attribute-level state aggregation in resource allocation [9], where the state is compressed into a low-dimensional summary that preserves enough information about future value to guide present decisions. Our structured surrogate fits within this lineage but is designed for allocation-dependent frontier growth: instead of compressing the frontier into a scalar size, it embeds each frontier individual into a nonnegative latent coverage vector and values the frontier by its aggregate coverage, which is what enables the closed-form Bellman backup of Section 3.

*Submodular optimization and greedy approximation.* Our per-round guarantee draws on submodular maximization, which provides a classical framework for reasoning about diminishing returns

in allocation and coverage problems. For monotone submodular maximization under a cardinality constraint, the greedy algorithm achieves the tight  $(1 - 1/e)$ -approximation [18]. Adaptive submodularity further extends greedy guarantees to sequential decisions with uncertain outcomes [11]. Our method exploits this perspective through a coverage-based future-value surrogate: for each fixed round budget, the surrogate objective is monotone with diminishing returns, yielding a  $(1 - 1/e)$ -approximation for the intra-round allocation; cross-round adaptivity is handled separately through the budget-conditioned future-value surrogate rather than by assuming adaptive submodularity of the full recruitment process.

## 5 Experiments

We evaluate GFP on a calibrated simulation environment designed to mirror real-world respondent-driven sampling. Section 5.1 introduces the simulation environment, calibrated to real-world public health dataset. Section 5.2 describes the four baselines we compare against. Section 5.3 specifies the episode protocol and evaluation metrics. Section 5.4 reports the empirical results.

### 5.1 Calibrated Simulation Environment

We evaluate all methods in a simulation environment whose structure mirrors real-world respondent-driven sampling. The environment’s covariate schema and inheritance probabilities are calibrated to the ICPSR 22140 respondent-driven sampling dataset, while the referral-capacity model is a parametric oracle.

Each individual is represented by a  $d = 72$ -dimensional one-hot covariate vector composed of  $K = 17$  categorical fields (demographic, behavioral, and socioeconomic attributes) derived from the ICPSR 22140 schema [16]. The oracle referral-capacity model is a Poisson model with covariate-dependent rates, calibrated so that the expected per-individual capacity matches an average degree  $\bar{\lambda} = 2.5$ , with a 5–10 $\times$  spread between the highest- and lowest-rate individuals so that uniform allocation is substantially suboptimal. The oracle covariate transition model is a categorical inheritance kernel: for each of the  $K$  covariate groups, the child independently inherits the parent’s category with a group-specific probability  $p_k$  (estimated from 73,669 recruiter–recruit dyads in ICPSR 22140; values range from  $p_{\text{SEX}} = 0.22$  to  $p_{\text{DRUGMAN}} = 0.98$ ), or is drawn uniformly otherwise. At the start of each episode the initial frontier  $\mathcal{F}_0$  is sampled uniformly with replacement from a pre-generated pool of  $N = 300$  random one-hot covariate vectors, with  $|\mathcal{F}_0| = 10$ . Full schema definitions, the inheritance-probability estimator, and all parametric details are deferred to Appendix C.1.

### 5.2 Baselines

We compare GFP against four baselines spanning random, reinforcement learning, and model-based dynamic-programming approaches.

*Random.* An unlearned baseline. At each round, it samples a round budget  $s_t$  uniformly from  $\{0, \dots, b_t\}$  and distributes the  $s_t$  units across frontier nodes by a single uniform multinomial draw.

*Budget-DQN.* A RL method that learns only the round-level spending decision. A Q-network scores each feasible round budget given the current state; the selected budget is then split across

frontier individuals by a fixed greedy allocator that prioritizes individuals with higher predicted recruitment counts. The budget decision and the individual-level allocation are decoupled.

*Factorized RL.* A RL method that factorizes the combinatorial allocation action into three learned decisions: (i) how much budget to spend, (ii) how many individuals to activate, and (iii) how to score each candidate individual. A DeepSets encoder maps the variable-size frontier into a fixed-dimensional state; a three-head Q-network produces budget Q-values,  $k$ -selection Q-values, and individual scores. At inference, the method selects the highest-value budget and  $k$ , picks the top- $k$  individuals by score, and distributes the budget via softmax allocation with integer rounding.

*IID-Population DP.* The model-based population-level method of [19]. It approximates future value using only the remaining budget and frontier size, fit by backward induction over a (budget, frontier size) table on top of a marginal Poisson PMF estimated from covariate samples drawn from the planning pool. Future value is therefore based on the number of future recruits but not their covariate composition.

### 5.3 Setup

The simulation environment defines the ground-truth dynamics, but planning algorithms do not have direct access to the oracle models at test time. Instead, learning-based methods are trained against learned surrogates  $q_\psi$  and  $G_\theta$  (the *planning environment*), while final evaluation is conducted under the oracle dynamics  $q^*, G^*$  (the *testing environment*). This separation ensures that performance comparisons are not confounded by differences in model fit. Full training data generation, model architectures, and hyperparameters are given in Appendix C.2.

*Episode protocol.* Each episode starts with  $|\mathcal{F}_0| = 10$ , a total budget  $B = 100$ , and a maximum horizon of 50 rounds. Episodes terminate early if the budget is exhausted or the frontier becomes empty. We evaluate across four discount factors  $\gamma \in \{0.9, 0.95, 0.99, 1.0\}$ . For each  $\gamma$ , every method uses that same discount factor internally, whether for training (the learning-based methods) or for backward induction and planning (the model-based methods).

*Metrics.* We report two episode-level metrics, averaged over 20 independent episodes per setting. The first is the final cumulative recruits  $\sum_t r_t$ , which measures total reach within a fixed budget and is the operational quantity public health agencies care about; we treat it as the headline metric. The second is the final discounted cumulative reward  $\sum_t \gamma^t r_t$ , a complementary measure that rewards both speed and quality.

### 5.4 Results

Table 1 reports final discounted reward and final cumulative recruits across the four discount factors; Figure 2 shows the per-round trajectories.

*GFP is best across all  $\gamma$ .* GFP attains the highest final discounted reward and the highest final cumulative recruits in all four settings. At  $\gamma = 1.0$ , GFP recruits  $99.5 \pm 0.2$  out of a budget of  $B = 100$ , leaving essentially no resources unconverted, while the next-best method,

**Table 1: Calibrated simulation environment,  $B = 100$ ,  $|\mathcal{F}_0| = 10$ ,  $n = 20$  eval episodes. Mean  $\pm$  standard error of the mean over episodes. Best per column in bold.**

	$\gamma=0.9$	$\gamma=0.95$	$\gamma=0.99$	$\gamma=1.0$
<i>Final discounted cumulative reward</i>				
Random	35.6 $\pm$ 3.9	37.4 $\pm$ 4.1	39.0 $\pm$ 4.3	39.4 $\pm$ 4.4
Budget-DQN	65.9 $\pm$ 2.7	68.4 $\pm$ 1.8	70.7 $\pm$ 1.6	72.4 $\pm$ 1.7
Factorized RL	57.9 $\pm$ 2.4	63.0 $\pm$ 3.8	85.4 $\pm$ 1.8	90.3 $\pm$ 2.7
IID-Population DP	79.4 $\pm$ 1.3	84.4 $\pm$ 1.2	88.9 $\pm$ 0.8	91.3 $\pm$ 1.0
GFP (ours)	<b>82.5<math>\pm</math>1.5</b>	<b>89.2<math>\pm</math>0.9</b>	<b>96.3<math>\pm</math>0.4</b>	<b>99.5<math>\pm</math>0.2</b>
<i>Final cumulative recruits</i>				
Random	39.4 $\pm$ 4.4	39.4 $\pm$ 4.4	39.4 $\pm$ 4.4	39.4 $\pm$ 4.4
Budget-DQN	72.9 $\pm$ 2.6	75.8 $\pm$ 1.9	71.9 $\pm$ 1.6	72.4 $\pm$ 1.7
Factorized RL	75.1 $\pm$ 2.8	85.2 $\pm$ 5.1	90.4 $\pm$ 1.8	90.3 $\pm$ 2.7
IID-Population DP	88.5 $\pm$ 1.0	89.3 $\pm$ 1.1	90.0 $\pm$ 0.8	91.3 $\pm$ 1.0
GFP (ours)	<b>94.5<math>\pm</math>1.0</b>	<b>97.0<math>\pm</math>0.6</b>	<b>98.6<math>\pm</math>0.3</b>	<b>99.5<math>\pm</math>0.2</b>

IID-Population DP, recruits  $91.3 \pm 1.0$ . The ordering of methods is stable across  $\gamma$ .

*Covariate composition matters.* IID-Population DP is the strongest baseline because it shares two design choices with GFP—budget-level dynamic programming and a frontier-value surrogate—but summarizes the frontier by its size alone. The residual gap between GFP and IID-Population DP (8.2 recruits at  $\gamma = 1.0$ , 6.0 at  $\gamma = 0.9$ ) therefore isolates the value of reasoning about covariate composition under covariate-dependent arrivals.

*RL baselines underperform.* Both RL baselines lag behind GFP and IID-Population DP because they do not exploit the structure of the problem and must learn from reward signal alone over a combinatorial action space, which is too large to explore effectively. Factorized RL narrows the gap at high  $\gamma$  (90.3 at  $\gamma = 1.0$ ) by factorizing the action, but still degrades at low  $\gamma$  (57.9 at  $\gamma = 0.9$ ); Budget-DQN further decouples the budget decision from individual-level allocation and underperforms across all  $\gamma$ .

*Early speed does not predict final performance.* Figure 2 shows that GFP is not the fastest method in early rounds: at  $\gamma = 1.0$ , IID-Population DP reaches  $\approx 90$  recruits within 4 rounds and Factorized RL also rises quickly, while GFP advances more deliberately and overtakes both methods only in later rounds. Methods that front-load recruitment can plateau below methods that pace their allocation, so the first-few-round ranking reverses by the end. GFP’s advantage comes from covariate-aware allocation: it matches units to covariate-conditioned referral capacity and prioritizes individuals whose offspring expand the frontier into less-covered regions of latent coverage space. IID-Population DP shares GFP’s budget-level dynamic programming but summarizes the frontier by size alone, and so cannot make either decision. Random allocation plateaus near 39.4 across all  $\gamma$ , confirming that allocation strategy, not budget size, is the dominant driver of recruitment.

## 6 Conclusion and Limitations

We studied adaptive multi-round allocation for peer-referral recruitment in respondent-driven sampling, where allocation decisions

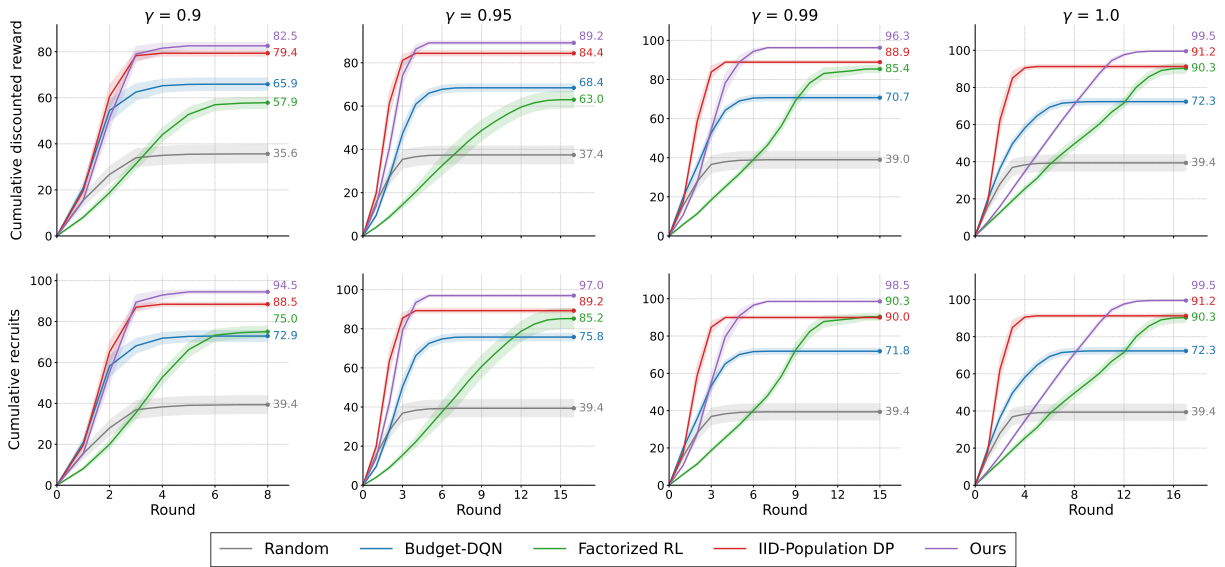


**Figure 2: Cumulative discounted reward (top) and cumulative recruits (bottom) per round across five methods, for  $\gamma \in \{0.9, 0.95, 0.99, 1.0\}$ . Lines are means over 20 episodes; bands are  $\pm 1$  SE.**

shape both immediate rewards and the covariate composition of future frontiers. We proposed *Generative Frontier Planning* (GFP), a model-based planner that combines a censored count model and a conditional diffusion model of offspring covariates with a latent coverage value surrogate. Under this surrogate, the expected future value depends on the diffusion model only through conditional Laplace embeddings of the offspring distribution that are amortized offline, yielding a deterministic Bellman backup; and the per-round objective is monotone with diminishing returns, giving a  $(1 - 1/e)$ -approximation guarantee for the intra-round allocation. On a simulation environment calibrated to the ICPSR-22140 respondent-driven sampling dataset, GFP outperforms random, reinforcement learning, and i.i.d. population-level dynamic-programming baselines across four discount factors, demonstrating its potential to extend the reach of peer-referral recruitment systems in public health.

*Limitations.* Our environment is calibrated to a real respondent-driven sampling dataset but is ultimately driven by a known oracle. Validating GFP on real recruitment data, ideally in partnership with a public health agency, is an important next step.

## Acknowledgments

This work was supported by ONR MURI N00014-24-1-2742.

## References

- [1] Dimitri P. Bertsekas. *Dynamic Programming and Optimal Control: Volume I*. Athena Scientific, 2012.
- [2] Dimitri P. Bertsekas. Neuro-dynamic programming. In *Encyclopedia of Optimization*. Springer, 2025.
- [3] Craig Boutilier and Tyler Lu. Budget allocation using weakly coupled, constrained markov decision processes. In *Proceedings of the Thirty-Second Conference on Uncertainty in Artificial Intelligence, UAI '16*, pages 52–61. AUAI Press, 2016.
- [4] Nicolas Carrara, Edouard Leurent, Romain Laroche, Tanguy Urvoy, Odalric-Ambrym Maillard, and Olivier Pietquin. Budgeted reinforcement learning in continuous state space. In *Advances in Neural Information Processing Systems*, volume 32. Curran Associates, Inc., 2019.
- [5] Saran Chen and Xin Lu. An immunization strategy for hidden populations. *Scientific reports*, 7(1):3268, 2017.
- [6] Dmitri Dolgov and Edmund Durfee. Computationally-efficient combinatorial auctions for resource allocation in weakly-coupled mdps. In *Proceedings of the Fourth International Joint Conference on Autonomous Agents and Multiagent Systems, AAMAS '05*, pages 657–664. Association for Computing Machinery, 2005.
- [7] Kousha Etessami, Alistair Stewart, and Mihalis Yannakakis. Polynomial time algorithms for branching markov decision processes and probabilistic min(max) polynomial bellman equations. *Mathematics of Operations Research*, 45(1):34–62, 2019.
- [8] Masih Fadaki, Sina Ansari, Ahmad Abareshi, and Paul Tae-Woo Lee. Sequential resource allocation for humanitarian operations using approximate dynamic programming. *Transportation Research Part E: Logistics and Transportation Review*, 201:104213, 2025.
- [9] Abraham George, Warren B Powell, and Sanjeev R Kulkarni. Value function approximation using multiple aggregation for multiattribute resource management. *Journal of Machine Learning Research*, 9(10), 2008.
- [10] Sharad Goel and Matthew J Salganik. Respondent-driven sampling as markov chain monte carlo. *Statistics in medicine*, 28(17):2202–2229, 2009.
- [11] Daniel Golovin and Andreas Krause. Adaptive submodularity: Theory and applications in active learning and stochastic optimization. *Journal of Artificial Intelligence Research*, 42:427–486, 2011.
- [12] Douglas D Heckathorn. Respondent-driven sampling: a new approach to the study of hidden populations. *Social problems*, 44(2):174–199, 1997.
- [13] Jonathan Ho, Ajay Jain, and Pieter Abbeel. Denoising diffusion probabilistic models. *Advances in neural information processing systems*, 33:6840–6851, 2020.
- [14] Akseli Kangaslahti, Davin Choo, Ling kai Kong, Milind Tambe, Alastair van Heerden, and Cheryl Johnson. Policy-embedded graph expansion: Networked hiv testing with diffusion-driven network samples. *International Joint Conference on Artificial Intelligence (IJCAI)*, 2026.
- [15] Nicolas Meuleau, Milos Hauskrecht, Kee-Eung Kim, Leonid Peshkin, Leslie Pack Kaelbling, Thomas Dean, and Craig Boutilier. Solving very large weakly coupled markov decision processes. In *Proceedings of the Fifteenth National Conference on Artificial Intelligence*, pages 165–172. AAAI Press, 1998.
- [16] Martina Morris and Richard Rothenberg. HIV Transmission Network Metastudy Project: An Archive of Data From Eight Network Studies, 1988–2001, 2011. ICPSR 22140.
- [17] Simon Munzert, Peter Selb, Anita Gohdes, Lukas F Stoetzer, and Will Lowe. Tracking and promoting the usage of a covid-19 contact tracing app. *Nature human behaviour*, 5(2):247–255, 2021.
- [18] G. L. Nemhauser, L. A. Wolsey, and M. L. Fisher. An analysis of approximations for maximizing submodular set functions—i. *Mathematical Programming*, 14:265–294,

1978.

- [19] Yuqi Pan, Davin Choo, Haichuan Wang, Milind Tambe, Alastair van Heerden, and Cheryl Johnson. Adaptive multi-round allocation with stochastic arrivals. In *International Conference on Machine Learning (ICML)*, 2026.
- [20] Warren B. Powell. *Approximate Dynamic Programming: Solving the Curses of Dimensionality*. John Wiley & Sons, 2007.
- [21] John N Tsitsiklis and Benjamin Van Roy. Feature-based methods for large scale dynamic programming. *Machine Learning*, 22(1):59–94, 1996.
- [22] Christina Winkler, Daniel Worrall, Emiel Hoogeboom, and Max Welling. Learning likelihoods with conditional normalizing flows. *arXiv preprint arXiv:1912.00042*, 2019.

## A Worked Example of the Latent Coverage Surrogate

To make the latent-coverage interpretation of Equation (3) concrete, consider a simplified setting in which each individual belongs to one of  $d$  categorical groups, and  $\mathbf{h}_\phi(\mathbf{x}) = \mathbf{e}_{\text{group}(\mathbf{x})}$  is the one-hot indicator of that group. Then  $z_j = \sum_{\mathbf{x} \in \mathcal{F}} h_{\phi,j}(\mathbf{x})$  counts the number of frontier individuals in group  $j$ , and  $F_\phi(r, \mathbf{z}) = \sum_j w_{\phi,j}(r)(1 - e^{-z_j})$  values the frontier by how many groups it covers, with diminishing marginal value as a given group becomes saturated. The general parameterization  $\mathbf{h}_\phi = \text{softplus}(\hat{\mathbf{h}}_\phi)$  generalizes this to  $d$  learned soft prototypes that need not align with observed categorical groups; the network learns which latent prototypes are worth covering.

## B Proofs

Throughout the proofs we use the notation introduced in the main text:  $p_{\psi,i}(\ell) = \mathbb{P}_{C \sim q_\psi(\cdot | \mathbf{x}_i)}(C \geq \ell)$  is the survival probability of the count model at threshold  $\ell$ ,

$$\alpha_{ij} = \alpha_{\theta,\phi,j}(\mathbf{x}_i) = \mathbb{E}_{\mathbf{y} \sim G_\theta(\cdot | \mathbf{x}_i)}[\exp(-h_{\phi,j}(\mathbf{y}))]$$

is the conditional Laplace embedding, and

$$\tau_{ij}(k_i) = \mathbb{E}_{C_i \sim q_\psi(\cdot | \mathbf{x}_i)}[\alpha_{ij}^{\min\{k_i, C_i\}}], \quad \tau_{ij}(0) = 1.$$

Recall the random next-frontier coverage  $\mathbf{Z}' = \sum_{\mathbf{x}' \in \mathcal{F}'} \mathbf{h}_\phi(\mathbf{x}')$  and its  $j$ -th coordinate  $Z'_j$ .

### B.1 Proof of Proposition 1

Fix a frontier  $\mathcal{F} = \{\mathbf{x}_1, \dots, \mathbf{x}_n\}$ , remaining budget  $r$ , round budget  $s \leq r$ , and allocation  $\mathbf{k} = (k_1, \dots, k_n)$  with  $\sum_i k_i = s$ . Since  $V_\phi(r - s, \mathcal{F}') = F_\phi(r - s, \mathbf{Z}')$  and  $F_\phi(r - s, \mathbf{z}) = \sum_j w_{\phi,j}(r - s)(1 - \exp(-z_j))$ , linearity of expectation gives

$$\mathbb{E}[V_\phi(r - s, \mathcal{F}')] = \sum_{j=1}^d w_{\phi,j}(r - s)(1 - \mathbb{E}[\exp(-Z'_j)]).$$

It therefore suffices to show that for every  $j$ ,

$$\mathbb{E}[\exp(-Z'_j)] = \prod_{i=1}^n \tau_{ij}(k_i). \quad (13)$$

For each parent  $i$ , let  $N_i = \min\{k_i, C_i\}$  be the number of offspring it generates, and let  $\{\mathbf{Y}_{i\ell}\}_{\ell=1}^{N_i}$  be those offspring, drawn i.i.d. from  $G_\theta(\cdot | \mathbf{x}_i)$ . Then

$$Z'_j = \sum_{i=1}^n \sum_{\ell=1}^{N_i} h_{\phi,j}(\mathbf{Y}_{i\ell}),$$

and by parent-wise independence of  $\{(C_i, \{\mathbf{Y}_{i\ell}\})\}_{i=1}^n$  given the current frontier and allocation,

$$\mathbb{E}[\exp(-Z'_j)] = \prod_{i=1}^n \mathbb{E}\left[\exp\left(-\sum_{\ell=1}^{N_i} h_{\phi,j}(\mathbf{Y}_{i\ell})\right)\right].$$

Fix a single parent  $i$  and condition on  $N_i$ . The offspring  $\{\mathbf{Y}_{i\ell}\}_{\ell=1}^{N_i}$  are i.i.d.  $G_\theta(\cdot | \mathbf{x}_i)$ , so

$$\begin{aligned} \mathbb{E}\left[\exp\left(-\sum_{\ell=1}^{N_i} h_{\phi,j}(\mathbf{Y}_{i\ell})\right) \middle| N_i\right] &= \prod_{\ell=1}^{N_i} \mathbb{E}_{\mathbf{y} \sim G_\theta(\cdot | \mathbf{x}_i)}[\exp(-h_{\phi,j}(\mathbf{y}))] \\ &= \alpha_{ij}^{N_i}. \end{aligned}$$

Taking expectation over  $N_i = \min\{k_i, C_i\}$  with  $C_i \sim q_\psi(\cdot \mid \mathbf{x}_i)$ ,

$$\mathbb{E} \left[ \exp \left( - \sum_{\ell=1}^{N_i} h_{\phi,j}(Y_{i\ell}) \right) \right] = \mathbb{E}_{C_i} \left[ \alpha_{ij}^{\min\{k_i, C_i\}} \right] = \tau_{ij}(k_i).$$

Substituting back into the previous display gives Equation (13), completing the proof.  $\square$

## B.2 Proof of Proposition 2

Decompose the surrogate as

$$f_s(\mathbf{k}) = A(\mathbf{k}) + \gamma \sum_{j=1}^d w_{\phi,j}(r-s) B_j(\mathbf{k}),$$

where

$$A(\mathbf{k}) = \sum_{i=1}^n \sum_{\ell=1}^{k_i} p_{\psi,i}(\ell), \quad B_j(\mathbf{k}) = 1 - \prod_{i=1}^n \tau_{ij}(k_i).$$

*Step 1: Bounds and basic monotonicity.* Since  $\mathbf{h}_\phi(\mathbf{x}) \in \mathbb{R}^d$ , we have  $h_{\phi,j}(\mathbf{y}) \geq 0$  and  $\exp(-h_{\phi,j}(\mathbf{y})) \in (0, 1]$ . Taking expectation under  $G_\theta(\cdot \mid \mathbf{x}_i)$  preserves the bound, so  $\alpha_{ij} \in (0, 1]$ . The map  $c \mapsto \alpha_{ij}^{\min\{k,c\}}$  is nonincreasing in  $k$  for every fixed  $c$ : increasing  $k$  to  $k+1$  leaves the term unchanged for  $c \leq k$  and multiplies it by  $\alpha_{ij} \in (0, 1]$  for  $c \geq k+1$ . Taking expectation under  $q_\psi$  preserves this, so  $\tau_{ij}(k_i)$  is nonincreasing in  $k_i$ , and  $\tau_{ij}(k_i) \in (0, 1]$ .

*Step 2: Monotonicity of  $f_s$ .* Increasing  $k_i$  by one adds  $p_{\psi,i}(k_i+1) \geq 0$  to  $A(\mathbf{k})$ . For each  $B_j$ , Step 1 implies the product  $\prod_{i'} \tau_{i'j}(k_{i'})$  is nonincreasing in  $k_i$ , so  $B_j(\mathbf{k})$  is nondecreasing in  $k_i$ . With  $w_{\phi,j}(r-s) \geq 0$  and  $\gamma \geq 0$ , this gives  $f_s(\mathbf{k} + \mathbf{e}_i) \geq f_s(\mathbf{k})$ .

*Step 3: Diminishing returns.* Fix  $\mathbf{k} \leq \mathbf{k}'$  coordinate-wise and any  $i$ . Since  $f_s$  is a nonnegative linear combination of  $A$  and  $\{B_j\}$ , it suffices to verify the diminishing-returns inequality

$$g(\mathbf{k} + \mathbf{e}_i) - g(\mathbf{k}) \geq g(\mathbf{k}' + \mathbf{e}_i) - g(\mathbf{k}'), \quad (14)$$

separately for  $g = A$  and  $g = B_j$  for each  $j$ .

*Term A.* The marginal contribution is  $A(\mathbf{k} + \mathbf{e}_i) - A(\mathbf{k}) = p_{\psi,i}(k_i + 1)$ . By assumption  $p_{\psi,i}$  is nonincreasing, so for  $k_i \leq k'_i$ ,  $p_{\psi,i}(k_i + 1) \geq p_{\psi,i}(k'_i + 1)$ , which is Equation (14) for  $A$ .

*Term  $B_j$*  (for the fixed  $j$  under consideration in the diminishing-returns inequality). Write  $u_j(\mathbf{k}) = \prod_{i'} \tau_{i'j}(k_{i'})$ . Then

$$B_j(\mathbf{k} + \mathbf{e}_i) - B_j(\mathbf{k}) = u_j(\mathbf{k}) \left( 1 - \frac{\tau_{ij}(k_i + 1)}{\tau_{ij}(k_i)} \right) = u_j(\mathbf{k}) \rho_i(k_i), \quad (15)$$

where  $\rho_i(k) := 1 - \tau_{ij}(k+1)/\tau_{ij}(k) \in [0, 1)$  and we have used  $\tau_{ij}(k_i) \in (0, 1]$  (Step 1). To establish Equation (14) for  $B_j$ , we show that both factors on the right-hand side of Equation (15) are point-wise larger at  $\mathbf{k}$  than at  $\mathbf{k}'$ .

*Step 3a:  $u_j(\mathbf{k}) \geq u_j(\mathbf{k}')$ .* Each factor  $\tau_{i'j}(k_{i'})$  is nonincreasing in  $k_{i'}$  (Step 1) and lies in  $(0, 1]$ . Since  $\mathbf{k} \leq \mathbf{k}'$  coordinate-wise,  $\tau_{i'j}(k_{i'}) \geq \tau_{i'j}(k'_{i'})$  for every  $i'$ , and multiplying nonnegative inequalities preserves the bound, giving  $u_j(\mathbf{k}) \geq u_j(\mathbf{k}')$ .

*Step 3b:  $\rho_i(k_i) \geq \rho_i(k'_i)$  when  $k_i \leq k'_i$ .* It suffices to show that  $\rho_i(k)$  is nonincreasing in  $k$ , equivalently that  $\tau_{ij}(k+1)/\tau_{ij}(k)$  is nondecreasing in  $k$ . Direct computation gives

$$\tau_{ij}(k+1) - \alpha_{ij} \tau_{ij}(k) = \mathbb{E} \left[ \alpha_{ij}^{\min\{k+1, C\}} - \alpha_{ij}^{1+\min\{k, C\}} \right],$$

where  $C \sim q_\psi(\cdot \mid \mathbf{x}_i)$ . Split the expectation by whether  $C \leq k$  or  $C \geq k+1$ :

- For  $C \geq k+1$ : both exponents equal  $k+1$  ( $\min\{k+1, C\} = k+1$  and  $1 + \min\{k, C\} = 1 + k = k+1$ ), so the integrand vanishes.
- For  $C \leq k$ :  $\min\{k+1, C\} = C$  and  $1 + \min\{k, C\} = 1 + C$ , so the integrand equals  $\alpha_{ij}^C - \alpha_{ij}^{1+C} = (1 - \alpha_{ij}) \alpha_{ij}^C \geq 0$ .

Combining,

$$\tau_{ij}(k+1) - \alpha_{ij} \tau_{ij}(k) = (1 - \alpha_{ij}) \mathbb{E} \left[ \alpha_{ij}^C \mathbf{1}\{C \leq k\} \right] =: g(k). \quad (16)$$

The function  $g(k)$  is nonnegative ( $\alpha_{ij} \leq 1$  and the indicator is nonnegative) and nondecreasing in  $k$  (the event  $\{C \leq k\}$  grows with  $k$ , and  $\alpha_{ij}^C \geq 0$ ). Rewriting Equation (16),

$$\frac{\tau_{ij}(k+1)}{\tau_{ij}(k)} = \alpha_{ij} + \frac{g(k)}{\tau_{ij}(k)}.$$

The numerator  $g(k)$  is nondecreasing in  $k$ , and the denominator  $\tau_{ij}(k)$  is nonincreasing in  $k$  and strictly positive (Step 1). Hence  $g(k)/\tau_{ij}(k)$  is nondecreasing in  $k$ , so  $\tau_{ij}(k+1)/\tau_{ij}(k)$  is nondecreasing in  $k$ , and  $\rho_i(k) = 1 - \tau_{ij}(k+1)/\tau_{ij}(k)$  is nonincreasing in  $k$ . In particular, for  $k_i \leq k'_i$ ,  $\rho_i(k_i) \geq \rho_i(k'_i)$ .

*Combining Steps 3a and 3b.* Both  $u_j(\mathbf{k}) \geq u_j(\mathbf{k}') \geq 0$  and  $\rho_i(k_i) \geq \rho_i(k'_i) \geq 0$  hold, so

$$u_j(\mathbf{k}) \rho_i(k_i) \geq u_j(\mathbf{k}') \rho_i(k'_i),$$

which by Equation (15) is Equation (14) for  $B_j$ .

Combining the cases  $g = A$  and  $g = B_j$  (for every  $j$ ) and using  $w_{\phi,j}(r-s) \geq 0$  and  $\gamma \geq 0$  yields the diminishing-returns inequality for  $f_s$ .  $\square$

## C Experimental Details

### C.1 Simulation Environment

*Covariate schema.* Table 2 lists the 17 categorical fields of the 72-dimensional one-hot covariate vector, derived from the ICPSR 22140 respondent-driven sampling dataset. Each field occupies a contiguous slice of the vector with exactly one active entry per group.

*Oracle referral-capacity model.* The oracle count model is a Poisson model with covariate-dependent rates. For an individual with covariate vector  $\mathbf{x} \in \{0, 1\}^{72}$ , the true referral capacity is

$$C_i \sim \text{Poisson}(\lambda(\mathbf{x}_i)), \quad \lambda(\mathbf{x}) = \kappa \cdot \text{softplus}(\mathbf{w}^\top \mathbf{x}),$$

where  $\mathbf{w} \in \mathbb{R}^{72}$  is a fixed weight vector drawn once from  $\mathcal{N}(\mathbf{0}, \sigma^2 \mathbf{I})$  and  $\kappa > 0$  is a calibration constant chosen so that the expected rate over uniformly random covariates equals a target mean degree  $\bar{\lambda}$ . We set  $\bar{\lambda} = 2.5$  and heterogeneity  $\sigma = 1.0$ , which induces a roughly 5–10 $\times$  spread between the highest- and lowest-rate individuals, making naive uniform allocation substantially suboptimal.

*Oracle covariate transition model.* Child covariates are generated from parent covariates via a categorical inheritance kernel. For each of the  $K = 17$  covariate groups, a child independently inherits the parent's category with a group-specific probability  $p_k$ ; otherwise the group is drawn uniformly at random:

$$x'_{\text{group}_k} \sim \begin{cases} \delta_{x_{\text{group}_k}} & \text{with probability } p_k, \\ \text{Uniform}(\{1, \dots, |\text{group}_k|\}) & \text{with probability } 1 - p_k. \end{cases}$$

**Table 2: The 17 categorical fields composing the 72-dimensional one-hot covariate vector.**

Field	Description	Size
LOCAL	Locality	4
RACE	Race	7
ETHN	Ethnicity	4
SEX	Sex	3
ORIENT	Sexual orientation	6
BEHAV	Sexual behavior	3
PRO	Sex-work profession	4
PIMP	Pimp status	4
JOHN	John status	4
DEALER	Drug dealing	4
DRUGMAN	Drug managing	4
THIEF	Theft	4
RETIRED	Retired	4
HWIFE	Homemaker	4
DISABLE	Disability	5
UNEMP	Unemployed	4
STREETS	Street-involved	4
Total		72

*Empirical inheritance probabilities.* Each  $p_k$  is estimated from 73,669 recruiter–recruit dyads in ICPSR 22140 (all disease subnetworks; NTYPE1=1, NTYPE2=3) via

$$p_k = \frac{\widehat{\text{match}}_k - 1/|\text{group}_k|}{1 - 1/|\text{group}_k|},$$

where  $\widehat{\text{match}}_k$  is the empirical fraction of dyads sharing the same category in group  $k$ , removing the agreement expected under independence. The resulting values are in Table 3.

**Table 3: Per-group empirical inheritance probabilities.**

Field	$p_k$
LOCAL	0.766
RACE	0.474
ETHN	0.861
SEX	0.223
ORIENT	0.744
BEHAV	0.762
PRO	0.573
PIMP	0.891
JOHN	0.680
DEALER	0.775
DRUGMAN	0.979
THIEF	0.940
RETIRED	0.960
HWIFE	0.861
DISABLE	0.865
UNEMP	0.339
STREETS	0.952

## C.2 Training Details

*Learned referral dynamics.* We fit the count model  $q_\psi$  on 2,048 censored triples  $(x_i, k_i, y_i)$ , generated by sampling covariates from the pool and allocations from  $\{1, \dots, 10\}$ . The Poisson rate is parameterized by a two-hidden-layer MLP with hidden dimension 64, ReLU activations, and a softplus output head, trained under the censored likelihood from Section 3.1 for 200 epochs. We fit the covariate model  $G_\theta$  on 4,096 parent–offspring covariate pairs drawn from the oracle transition kernel, instantiated as a conditional DDPM [13] and trained for 200 epochs. Its noise predictor is a three-hidden-layer MLP with hidden dimension 512 and GELU activations, conditioned on the parent covariate, the noised offspring covariate, and a 16-dimensional sinusoidal time embedding. Since the covariates are discrete, we recover offspring categories from the continuous samples by rounding, following prior work [14].

*Reinforcement learning baselines.* We train Budget-DQN and Factorized RL for 500 episodes each in the planning environment. Both share the same training configuration: a replay buffer of capacity 10,000, batch size 32, hidden dimension 64, learning rate  $10^{-3}$ , and discount factor  $\gamma$  matched to the evaluation setting. Budget-DQN encodes the frontier with a DeepSets module and feeds the resulting embedding to a two-hidden-layer Q-network over total round budgets. Factorized RL uses the same DeepSets encoder followed by three two-hidden-layer Q-heads, one each for budget, support size, and individual scoring, with  $\epsilon$ -greedy exploration linearly decayed from 0.20 to 0.05 over training.

*GFP training.* The frontier-value surrogate uses latent dimension  $d = 32$  and hidden dimension 64, with the covariate coverage network instantiated as a two-hidden-layer MLP and the budget-weight network as a one-hidden-layer MLP. The amortized Laplace network  $L_\eta$  is a two-hidden-layer MLP with hidden dimension 64 and output dimension  $d$ . We train  $L_\eta$  for 200 gradient steps on 256 parent covariates with 64 offspring samples per parent (Adam, learning rate  $10^{-3}$ , batch size 128), and refresh it once before value training begins. The value surrogate is then trained by fitted value iteration for 200 iterations with batch size 16 and learning rate  $10^{-3}$ , using a pool of 256 (frontier, budget) states collected from 64 random rollouts in the planning environment.

*IID-Population DP [19].* The baseline computes a population-level future-value table by fitting a marginal Poisson PMF from 1,024 covariate samples drawn from the planning pool, then running standard backward induction over (budget, frontier size) pairs up to the full budget  $B$ .



